

## DOCUMENTATION PAGE

1a. REPORT CLASSIFICATION Unclassified			1b. RESTRICTIVE MARKINGS			
2a. SECURITY CLASSIFICATION AUTHORITY			3. DISTRIBUTION / AVAILABILITY OF REPORT Approved for public release; distribution unlimited			
2b. DECLASSIFICATION / DOWNGRADING SCHEDULE						
4. PERFORMING ORGANIZATION REPORT NUMBER(S) MDC Q1296			5. MONITORING ORGANIZATION REPORT NUMBER(S) AFOSR-TR- 87-1476			
6a. NAME OF PERFORMING ORGANIZATION McDonnell Douglas Research Laboratories		6b. OFFICE SYMBOL (if applicable)	7a. NAME OF MONITORING ORGANIZATION AFOSR/NA			
6c. ADDRESS (City, State, and ZIP Code) P. O. Box 516 St. Louis, MO 63166			7b. ADDRESS (City, State, and ZIP Code) Bolling Air Force Base Washington, DC 20332			
8a. NAME OF FUNDING / SPONSORING ORGANIZATION Department of the Air Force		8b. OFFICE SYMBOL (if applicable) AFOSR/NA	9. PROCUREMENT INSTRUMENT IDENTIFICATION NUMBER F49620-83-C-0048			
8c. ADDRESS (City, State, and ZIP Code) Air Force Office of Scientific Research/AFOSR Bolling Air Force Base Washington, DC 20332			10. SOURCE OF FUNDING NUMBERS	PROGRAM ELEMENT NO. 61102 F	PROJECT NO. 2307	TASK NO. A2
			WORK UNIT ACCESSION NO.			
11. TITLE (Include Security Classification) ACTIVE CONTROL OF JET FLOWFIELDS						
12. PERSONAL AUTHOR(S) Kibens, Valdis and Wlezien, Richard W.						
13a. TYPE OF REPORT Final Technical		13b. TIME COVRED FROM 83 Jan 1 TO 85 Dec 31	14. DATE OF REPORT (Year, Month, Day) 1987 June 29		15. PAGE COUNT 33	
16. SUPPLEMENTARY NOTATION						
17. COSATI CODES			18. SUBJECT TERMS (Continue on reverse if necessary and identify by block number)			
FIELD	GROUP	SUB-GROUP	Fluid mechanics, Passive control, Control of turbulence, Shear layers, Active control, Asymmetric nozzles Jet flows, Image processing, Slanted nozzles			
19. ABSTRACT (Continue on reverse if necessary and identify by block number) Passive and active control of jet shear layer development were investigated as mechanisms for modifying the global characteristics of jet flowfields. Slanted and stepped "indeterminate origin" (I.O.) nozzles were used as passive, geometry-based control devices which modified the flow origins. Active control techniques were also investigated, in which periodic acoustic excitation signals were injected into the I.O. nozzle shear layers. Flow visualization techniques based on a pulsed copper-vapor laser were used in a phase-conditioned image acquisition mode to assemble optically averaged sets of images acquired at known times throughout the repetition cycle of the basic flow oscillation period. Hot wire data were used to verify the effect of the control techniques on the mean and fluctuating flow properties. The flow visualization images were digitally enhanced and processed to show locations of prominent vorticity concentrations. Three-dimensional vortex interaction patterns were assembled in a format suitable for movie mode on a graphic display workstation, showing the evolution of three-dimensional vortex systems in time.						
20. DISTRIBUTION / AVAILABILITY OF ABSTRACT <input checked="" type="checkbox"/> UNCLASSIFIED/UNLIMITED <input type="checkbox"/> SAME AS RPT <input type="checkbox"/> DTIC USERS			21. ABSTRACT SECURITY CLASSIFICATION Unclassified			
22a. NAME OF RESPONSIBLE INDIVIDUAL James M. McMichael			22b. TELEPHONE (Include Area Code) (202) 767-4935		22c. OFFICE SYMBOL AFOSR/NA	

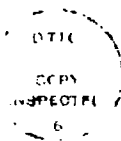
DTIC  
ELECTE  
S  
OCT 27 1987  
D  
E

REPORT DOCUMENTATION PAGE - Continued

18. SUBJECT TERMS - Continued

Indeterminate origin nozzles, Stepped nozzles  
Pulsed laser flow visualization

Accession For	
NTIS GRA&I	<input checked="" type="checkbox"/>
DTIC TAB	<input type="checkbox"/>
Unannounced	<input type="checkbox"/>
Justification	
By _____	
Distribution/	
Availability Codes	
Dist	Avail and/or Special
A-1	



## PREFACE

The work reported herein was performed by the McDonnell Douglas Research Laboratories in St. Louis, Missouri, for the United States Air Force Office of Scientific Research, Bolling Air Force Base, Washington, DC, under Contract F49620-83-C-0048. The work reported was conducted from 1 January 1983 to 1 January 1986 in the Flight Sciences Department, managed by Dr. R. J. Hakkinen. The principal investigator was Dr. V. Kibens; Dr. R. W. Wlezien was co-investigator. The program technical monitor was Dr. James M. McMichael.

This technical report has been reviewed and approved.



---

R. J. Hakkinen  
Director-Research, Flight Sciences  
McDonnell Douglas Research Laboratories



---

D. P. Ames  
MDC Distinguished Fellow -  
General Manager  
McDonnell Douglas Research Laboratories

## TABLE OF CONTENTS

Section	Page
1. INTRODUCTION.....	1
2. OBJECTIVES.....	3
3. ACTIVE-CONTROL INVESTIGATION.....	5
3.1 Flow System and Data Processing.....	5
3.2 Nozzle Geometry.....	6
3.3 Excitation Techniques.....	6
3.4 Phase-Conditioned Schlieren System.....	8
3.5 Results.....	10
3.5.1 Reference Nozzle.....	10
3.5.2 Category I - Continuous I.O. Nozzles.....	12
3.5.3 Category II - Discontinuous I.O. Nozzles.....	17
4. INVESTIGATION OF SHEAR LAYER STRUCTURE.....	25
4.1 Image Acquisition.....	25
4.2 Image Processing.....	26
4.3 Image Display.....	29
5. DISCUSSION AND CONCLUSIONS.....	30
6. PUBLICATIONS AND PRESENTATIONS.....	31
6.1 Publications.....	31
6.2 Presentations.....	31
7. REFERENCES.....	33

## LIST OF ILLUSTRATIONS

Figure		Page
1.	Geometry designations for (a) inclined and (b) stepped I.O. nozzles.....	7
2.	Acoustic excitation apparatus for (a) stepped and (b) inclined nozzles.....	8
3.	Conditioning criteria for schlieren video.....	9
4.	Reference nozzle 1A; U=25 m/s. plenum excitation, $f_{ex} = 3344$ Hz. Flash triggered on $f_{ex}/8$ : (a) $\phi=0^\circ$ , (b) $\phi=90^\circ$ , (c) $\phi=180^\circ$ , and (d) $\phi=270^\circ$ .....	11
5.	Nozzle 1C; U=30 m/s, lip excitation: $f_{ex} = 1390$ Hz. (a) Side view and (b) view from $\psi=0^\circ$ (bottom).....	13
6.	Nozzle 1C; U=30 m/s, lip excitation: $f_{ex} = 5230$ Hz.....	14
7.	Nozzle 2D; U=25 m/s, helium chamber excitation: $f_{ex} = 364$ Hz....	15
8.	Nozzle 2D; U=20 m/s, helium chamber excitation: $f_{ex} = 340$ Hz....	16
9.	Nozzle 2D; U=20 m/s, helium chamber excitation: $f_{ex} = 450$ Hz....	16
10.	Nozzle 2E; U=15 m/s, plenum excitation: $f_{ex} = 475$ Hz.....	17
11.	Nozzle 1E; U=15 m/s, plenum excitation: $f_{ex} = 1078$ Hz.....	18
12.	Nozzle 2G; U=15 m/s, plenum excitation: $f_{ex} = 266$ Hz.....	18
13.	Nozzle 1G; U=15 m/s, lip excitation: $f_{ex} = 1199$ Hz: (a) with splitter plate and (b) without splitter plate.....	19
14.	Nozzle 1G; U=15 m/s, lip excitation: $f_{ex} = 680$ Hz.....	20
15.	Step nozzle; U=15 m/s; lip excitation frequency $f_{ex} = 985$ Hz, $Re=23\ 000$ : (a), (b), and (c) are three realizations of flow-fields that meet identical conditioning criteria.....	21
16.	Nozzle 1G; U=15 m/s, lip excitation, upper sector only: $f_{ex} = 428$ Hz. (a) Side view and (b) view from $\psi=0^\circ$ (bottom).....	22
17.	Nozzle 1G; U=15 m/s, lip excitation, upper section only: $f_{ex} = 411$ Hz.....	22
18.	Nozzle 1G; U=15 m/s, lip excitation, upper and lower sectors $180^\circ$ out of phase: $f_{ex} = 411$ Hz.....	23
19.	Nozzle 1G; u=15 m/s, lip excitation, upper sector only: $f_{ex} = 411$ Hz, $x/D=4.0$ . (a) Mean-velocity distribution and (b) momentum-thickness distribution.....	24

**LIST OF ILLUSTRATIONS**  
(continued)

Figure		Page
20.	Three-dimensional reconstruction of vortex lines.....	25
21.	Shear-layer composite excitation.....	26
22.	Pulsed-laser flow visualization.....	27
23.	Equalized image of seeded jet: $U_0=22.5$ m/s; $f_{ex}=1736, 434$ .....	27
24.	Local histogram equalization technique.....	28
25.	Vortex detection.....	28
26.	Vortex track diagram; axisymmetric jet.....	28

## 1. INTRODUCTION

This report describes results of research conducted during the second and third years of the contract. Together with AFOSR document TR-84-0551, (Ref. 1), which covers the first year's work, this report describes the results of the investigation entitled "Control of Jet Flowfield Dynamics."

The first year of the program (Refs. 1 and 2) dealt with passive turbulence control techniques applied to subsonic, round jets of ambient-temperature air. Variation of nozzle exit shapes and the consequent effect of shape on inherent flow instabilities constituted the principal control mechanism for manipulating jet development.

Indeterminate origin (I.O.) nozzles with slanted, stepped, and crenelated exits were used to generate and passively control jet shear layers formed under a variety of initial flow conditions. Extensive flow-visualization and hot-wire surveys revealed a variety of distinct dynamic-instability modes which resulted from the geometries selected over the velocity range  $4 \leq U \leq 40$  m/s. The response of the constant-phase lines of the instability waves to the geometry of the nozzle termination was the principal criterion used to categorize the instability modes. A slight departure of the slant of the nozzle exit from the normal to the flow direction caused an identical change in the slant angle between the original flow and the early instability waves. As either the slant angle of the nozzle exit or the stream velocity was increased, the orientation of the instability waves with respect to the slant of the origin became more tenuous, until the instability wave finally became normal to the flow direction. Stepped nozzles showed a reconciling of vortex lines originating from adjacent trailing-edge segments at different streamwise positions.

The streamwise scale development was surveyed by spectrally mapping the hot-wire anemometer signals. The results confirmed that the observed distortion of the mean properties of the jet spreading was related to the interaction of the azimuthally varying instability wave patterns generated by the particular I.O. nozzle geometry.

Work described in the present report extended the application of control to include active techniques; such techniques add excitation energy from external sources as perturbations to the shear layers that form the origin of the jet. The objective of the research was to develop methods for controlling

near-field fluctuating pressures and thus to reduce the sonic fatigue impact of jets, to reduce the acoustic and infrared signatures of aircraft and missiles, and to improve the mixing efficiency of ejector nozzles by suitably matching control signal characteristics, nozzle exit geometry, and jet flow-field parameters.

The investigation of jet shear-layer control is part of a continuing MDRL effort to develop techniques for modifying complex, unsteady flows. Either enhancement or suppression of flow characteristics pertaining to a particular application may be required. The approach chosen is data-intensive, using computer-controlled apparatus and data surveying techniques. The approach involves global flow-visualization methods and image processing, as well as detailed hot-wire, LDV, and microphone surveys.

## 2. OBJECTIVES

The principal objectives of the program were to observe and characterize the three-dimensional effects of indeterminate origin (I.O.) nozzles by use of flow visualization to obtain qualitative data and use of computer-controlled hot-wire measurements for quantitative description of the flowfield development.

The specific objectives of the second and third years of the program centered on the implementation of active and interactive control concepts.

The second-year objectives were the following:

1. Select and evaluate the efficiency of acoustical and mechanical excitation devices for introducing active control signals into jet flowfields, by use of existing MDRL exciter designs for axisymmetric jets.
2. Perform a detailed flowfield measurement test sequence of selected acoustically excited jets by use of the I.O. nozzles developed earlier in the contract research program.
3. Perform additional tests to evaluate control effectiveness of exciter systems by use of conditional sampling algorithms triggered by suitably phased pulses derived from the signals that actuate the excitation devices.
4. Install an ejector shroud at the end of a constant-diameter nozzle-extension pipe forced by an acoustic nodal-point pipe resonance exciter. Evaluate maximum positive control obtainable.
5. Select nozzle and exciter combinations that achieve the highest degree of amplifying and attenuating dynamic flowfield control for experiments in interactive control.

The initial objectives were modified as work progressed to reflect the impact of the new active-control results. Acoustic excitation devices were built for slanted and stepped nozzles (see description in Section 2.2). Flow-visualization tests showed that acoustic excitation produced a great variety of vigorous three-dimensional vortex interactions in the flowfields, which resulted in spreading rates and jet asymmetries that exceeded those observed under passive-control conditions. It was decided to refocus the program on the detailed vortex interactions observed in selected actively controlled flowfields. The new direction required development of an experimental technique for investigating the detailed motion of interacting vortices under the

influence of acoustic forcing. This technique used a phase-locked conditional video schlieren system for optically averaging flowfield motion as a function of the phase angle of the underlying periodicity of the flowfield.

Accordingly, the modified objectives for the second year of the program were as follows:

1. Same as above.
2. Develop an optical sampling and averaging system consisting of a schlieren system, a standard video camera and monitor, a white-light high-intensity strobe light, and an analog logic circuit for deriving the flash triggering pulse from a flowfield microphone signal and the excitation pulse train, synchronized with the scan rate of the video system.
3. Obtain representative flow visualization data photographically and on video tape for the geometry, excitation frequency, and jet velocity matrix using the phase-conditioned optical system.
4. Perform hot-wire measurements characterizing the global flowfield features for selected high-activity cases.

The initial third-year objectives were to develop interactive control techniques and to apply them to the I.O. nozzle flowfields. These objectives were replaced by an extension of the direction described above. The output of the phase-conditioned flow-visualization system was a systematically ordered set of ensemble-averaged images in ascending order of the phase angles of the driving process. The new objective was to start using image-processing techniques in conjunction with the sets of visualization images to determine trajectories and merging patterns of the systems of vortices generated by active-control excitation of jets from I.O. nozzles.

### 3. ACTIVE-CONTROL INVESTIGATION

The work described follows MDRL research described in Refs. 1 and 2, as well as other investigations that demonstrate effects of initial jet geometry on jet flowfields. The other investigations include those by Husain and Hussain<sup>3</sup> and Gutmark and Ho<sup>4</sup> in which spreading characteristics of elliptic jets are shown to be significantly changed by distortion of the nozzle exit shape. Experiments by Krothapalli et al.<sup>5</sup> demonstrate related effects for rectangular jets. Three-dimensionality of the origin has been investigated by Breidenthal,<sup>6</sup> who used a splitter plate with a tabbed trailing edge as the origin of a two-dimensional mixing layer. Lee and Reynolds<sup>7</sup> perturbed the jet origin by applying streamwise pulsation of the flow and simultaneous rotational displacement of the nozzle; a dramatic three-dimensionalization of vortex interactions was achieved. The complexity of generation and subsequent interaction of three-dimensional vortex systems has also been demonstrated by Rockwell<sup>8</sup> and Smith.<sup>9</sup>

Our work describes properties of flowfields from I.O. nozzles under active control, i.e., those influenced by externally powered perturbations injected into the flows to enhance or suppress naturally occurring instability wave patterns. Most of the results are presented as flow-visualization photographs taken with a phase-conditioned schlieren system that images instantaneous or phase-averaged photographs of flowfield activity when specific criteria are satisfied.

#### 3.1 Flow System and Data Processing

Experiments were performed with a flow system supplied from a high-pressure centrifugal blower with speed stabilized by feedback control. In the experiments 24.5- and 63.5-mm-diameter nozzles were used to generate subsonic flows with low disturbance levels. Flow rates were controlled by computer. Hot-wire data were obtained with a three-degree-of-freedom, computer-controlled traverse and processed through a minicomputer data acquisition system. Nozzles were installed at the exit of a bi-cubic contraction, along with a specially designed injector located immediately upstream of the nozzle exit. To provide density gradients for schlieren photography, helium was supplied from a central distribution point through four separate tubes into the injection chamber. The helium was introduced into the boundary layer

through a downstream-pointing injection slit. This technique provides more effective visualization of shear-layer features than techniques which introduce smoke or helium into the entire flowfield.

### 3.2 Nozzle Geometry

The I.O. nozzles are depicted in Fig. 1. The inclined and stepped geometries are denoted by letters C - H, which designate the length of nozzle extension with respect to the nozzle virtual origin; the origins are indicated by dashed circles. Nozzles of 25.4- and 63.5-mm diameter are designated series 1 and 2, respectively. The azimuth angle is referenced to  $\psi = 0^\circ$ , taken as the center of the nozzle lip sector with farthest downstream extension, as shown in Fig. 1. The upstream section of all nozzles is an axisymmetric, constant-diameter pipe which is 2.5 diameters (D) in length from the end of the contraction to the virtual origin. This arrangement ensures that the boundary-layer thickness is identical for nozzles in the same series.

### 3.3 Excitation Techniques

Externally powered acoustic perturbations were introduced through three excitation techniques. In the first technique, external exciters were constructed for the inclined and stepped nozzles, 1C and 1G, in the form of wrap-around, segmental chambers, as shown in Fig. 2. The sound impinges on the shear layer as it leaves the nozzle lip. The excitation chambers are divided into four subchambers, each driven independently through its inlet port; they can be driven from one or more acoustic drivers. Driver amplifiers are controlled from multiple phase-locked signal generators. Thus the frequency, amplitude, and phase relationships among the driving waveforms can be independently controlled and the upper and lower shear-layer sectors for the stepped nozzle can be excited separately. The external-lip excitation technique was limited to the two nozzles, 1C and 1G, for which excitation devices were built.

To apply excitation to other nozzle terminations, two additional means of excitation were devised. The first consisted of introducing acoustic perturbations into the helium injection chamber, thereby perturbing the boundary layer passing over the injection slit. This technique was effective in perturbing the shear layer, but left in question the exact nature of the perturbations and their means of transport to the nozzle lip. To answer these ques-

$\frac{n}{4}$	Designation	
	Inclined nozzle	Stepped nozzle
4	C	F
2	D	G
1	E	H

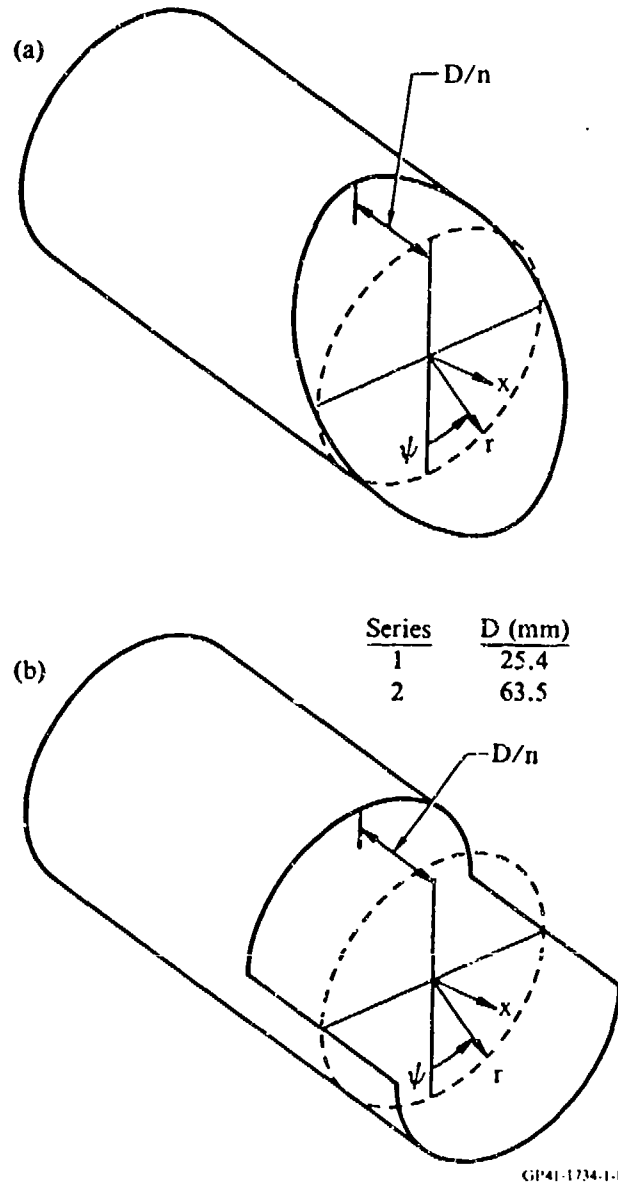
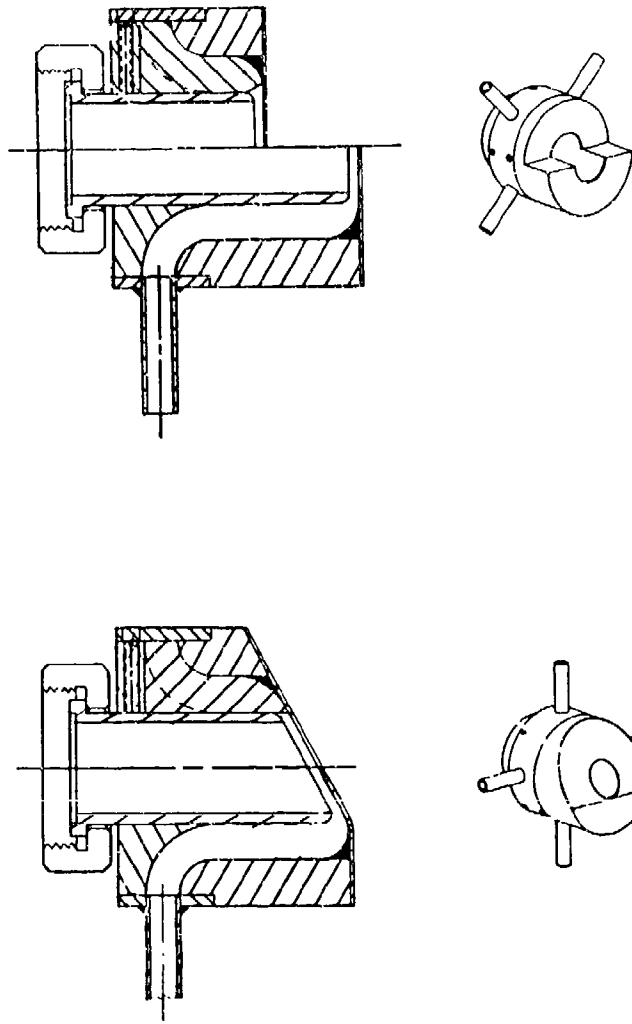


Fig. 1 Geometry designations for (a) inclined and (b) stepped I.O. nozzles.

tions, a second excitation technique introduced the signal into the plenum chamber at a location about 2 m upstream from the nozzle exit. The excitation levels were selected for maximum effect at the nozzle exit. As a rule, excessive excitation amplitudes reduced gross shear-layer spreading rates. No attempt was made to engage chamber resonances.



CP41-1734-2-R

**Fig. 2 Acoustic excitation apparatus for (a) stepped and (b) inclined nozzles.**

**3.4 Phase-Conditioned Schlieren System**

Excitation enabled acquisition of visualization images on the basis of specific flow features. A multiple-conditioned schlieren system was developed for this purpose; a conditionally triggered strobe light was used as the light source. The schlieren field was imaged by a black-and-white video camera, displayed on a video monitor, and recorded on videotape.

Conditioning criteria for image selection are shown in Fig. 3. A strobe trigger pulse was generated by the conditioning circuitry when three criteria were sequentially satisfied. The first criterion required the presence of the

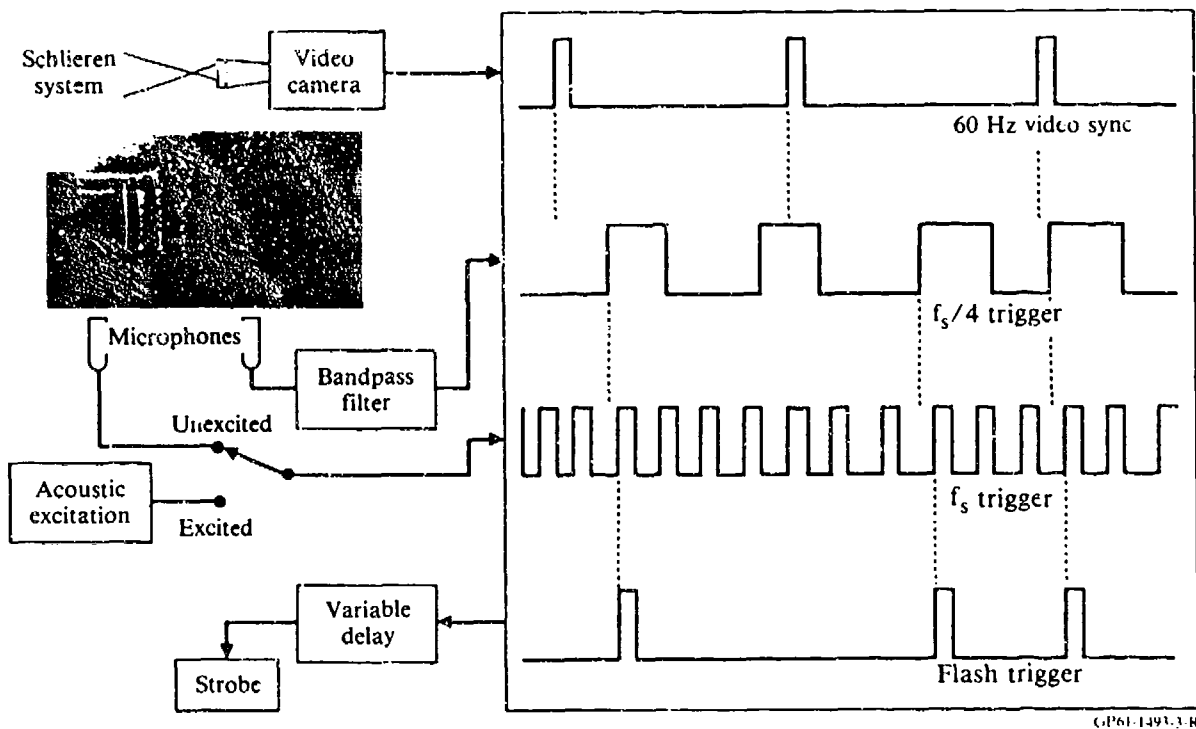


Fig. 3. Conditioning criteria for schlieren video. ( $f_s$  = shear layer instability frequency).

video synchronization pulse, which signified the beginning of a video scan at 60 hertz. The second criterion was based on a shear-layer subharmonic frequency sensed by a near-field microphone. The microphone signal was bandpass-filtered around a frequency chosen with a real-time spectrum analyzer. When the filtered signal activated a zero-crossing detector, a pulse was generated to indicate that the criterion had been met. The third criterion required the flash to be keyed to the fundamental excitation pulse immediately after the second criterion was satisfied.

Triggering image selection on the fundamental excitation pulses minimized the influence of the jitter of the subharmonic signal caused by uncertainty in the location of pairing events that constitute subharmonic generation. An additional effect of introducing the third criterion was to phase-lock the entire sequence of pairings that generated the large scales to which the second criterion was keyed. A variable delay allowed the schlieren source to be flashed at an arbitrary phase of the subharmonic that was used in the second triggering criterion. The subharmonic normally selected was the lowest excitation frequency submultiple for which a spectrum peak could be detected. The effectiveness of image conditioning and selection decreases with the

sharpness and level of the spectrum peak of the subharmonic being detected. The multiple-conditioning system can also be used for an unexcited flow. For that case, the third criterion was supplied by an external microphone, which sensed the initial instability frequency of the shear layer.

Since the flash duration was only 20 ns, the technique depended on the image persistence of the video camera to generate a viable video presentation. An alternative means of recording images, used for figures in this report, was with a standard 35-mm camera, black-and-white film, and use of the conditioning circuit in a single-flash mode. Optical-ensemble averages of a series of images may be photographed from the monitor or recorded directly onto 35-mm film.

### 3.5 Results

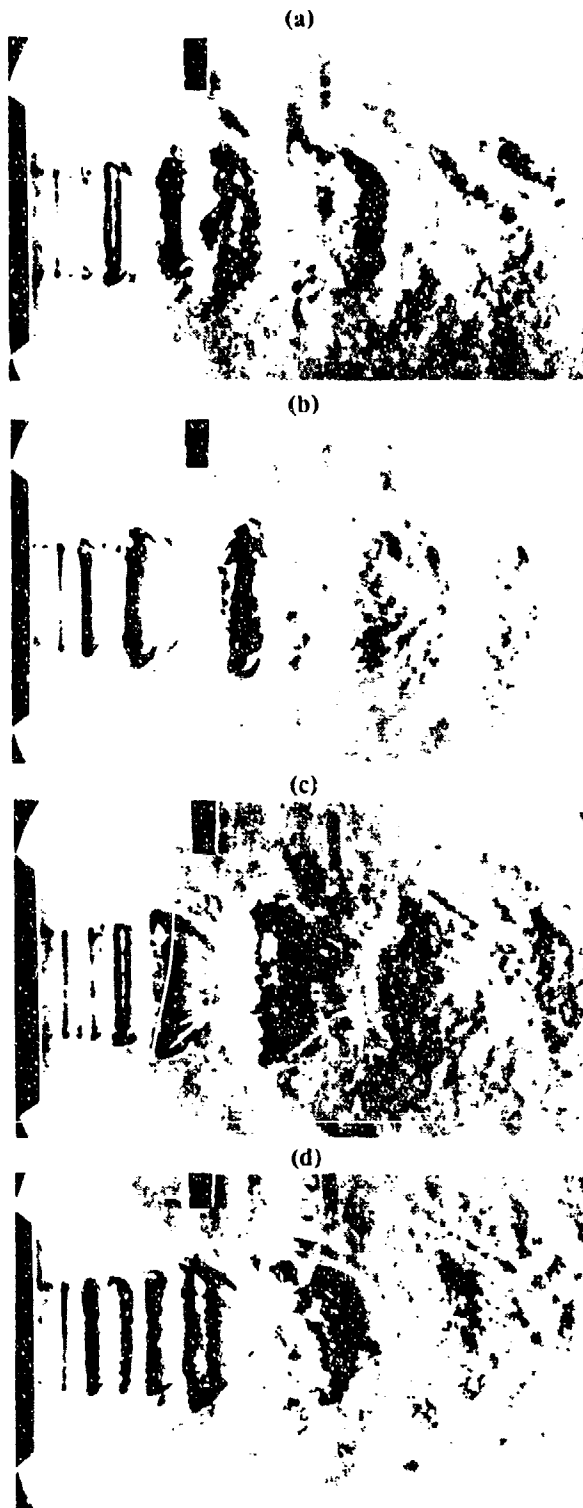
The phase-conditioned schlieren technique, in conjunction with boundary-layer helium injection, permits detailed observation of quasi-periodic flow-field motion when the triggering flash delay is slowly varied. As the phase is changed, the sequence of video images presents a slow-motion view of vorticity concentration interactions throughout the flowfield.

Since the observed flow features are periodic, nonsymmetrical nozzles may be rotated for a synchronized presentation of views from arbitrary azimuthal positions. The second conditioning criterion can select any of the detectable subharmonics; therefore, the details of motion visualized can be keyed to a full cycle of any of the subharmonics found in the flowfield. Still photographs taken with black-and-white film, although of higher resolution, present much less information than that available from videotape.

#### 3.5.1 Reference Nozzle

The four images in Fig. 4 show flowfield development for the circular reference nozzle 1A at velocity  $U = 25$  m/s. The nozzle used in this figure was described by Kibens in Ref. 10.

Plenum excitation was applied at 3344 Hz, the natural instability frequency of the shear layer. The strobe was triggered on the third subharmonic of the excitation frequency,  $f_{ex}/8$ . The spectrum of the signal obtained by the microphone, which is seen in the photographs as a black vertical rod, showed sharp peaks at the fundamental harmonic and three subharmonics. Phase values in the sequence of photographs differ by  $90^\circ$  and refer to one cycle of



87-222-269

Fig. 4 Reference nozzle 1A;  $U = 25$  m/s, plenum excitation,  $F_{ex} = 3344$  Hz. Flash triggered on  $f_{ex}/8$ : (a)  $\phi = 0^\circ$ , (b)  $\phi = 90^\circ$ , (c)  $\phi = 180^\circ$ , and (d)  $\phi = 270^\circ$ .

large-scale motion corresponding to  $f_{ex}/8$ . Therefore, the smallest scales in the flow correspond to the excitation signal at 3344 Hz and are visible at the exit of the exciter. The full cycle depicted in the sequence of photographs includes eight periods of the excitation signal. The double structure directly below the microphone in Fig. 4(a) at  $\phi = 0^\circ$  has moved slightly downstream with respect to the microphone in Fig. 4(b). It is still farther downstream in Fig. 4(c) for  $\phi = 150^\circ$ , and for 4(d) the cycle is almost complete. The next photograph in the sequence is 4(a).

This sequence of photographs documents the strong tendency of the vortex pairing system toward axial symmetry which persists well past the end of the potential core in the large-scale flow structures. This observation is further confirmed when the axisymmetric reference flow is compared to flows from I.O. nozzles, which exhibit a wide range of three-dimensional, nonaxisymmetric vorticity concentration patterns. The pairing process has the effect of attenuating local asymmetries and regenerating axial symmetry by orienting the vortex pairing system perpendicular to the vorticity vector which represents the mean shear. Roshko has pointed out (Ref. 11) that in two-dimensional shear layers the tendency for the generation of three-dimensionality by secondary instabilities is suppressed at pairing locations and a strong reorganizing effect is imposed by the primary pairing process. The following sections, as well as Ref. 1, illustrate the key effect in the control concept: even very slight departures from the axisymmetric reference configuration in terms of geometry or excitation parameters can introduce major changes in development of shear-layer vortex structures. Particular geometries and excitation parameters can be selected to modify global shear-flow properties.

### 3.5.2 Category I - Continuous I.O. Nozzles

Small departures of exit slant angle from perpendicular to the stream direction are expected to result in flows that are qualitatively related to the reference flow described in Fig. 4. Our work on passive control (Refs. 1 and 2), identified two general classes of shear-layer instability waves: 1) the continuous vortex-line instability wave systems for which the nozzle lip-line geometry determines the phase relationship of the initial wave fronts, and 2) the class of locally coherent instabilities for which characteristics of the wave system are determined primarily by the shear-layer sector leaving the nozzle at the farthest upstream point. Subsequent development

of constant-phase lines is keyed to the shear-layer sector that first becomes unstable. As noted by Roshko (Ref. 11), introduction of three-dimensionality at the origin counteracts the tendency of shear layers to establish instability waves with wave fronts parallel to the mean vorticity. If the jet shear layer were to be unwrapped, then the nozzle slant angle would represent the discrepancy between the constant-phase lines that develop parallel to the lip line and the mean shear vorticity vector of the jet flow.

Figure 5 presents two views of flow from nozzle 1C with external excitation. Initially, phase fronts are parallel to the nozzle exit and pairing occurs in the plane of the nozzle exit. This flow is an example of a continuous-vortex-line instability system, although subsequent vortex interactions indicate a tendency toward generation of vortex systems that orient

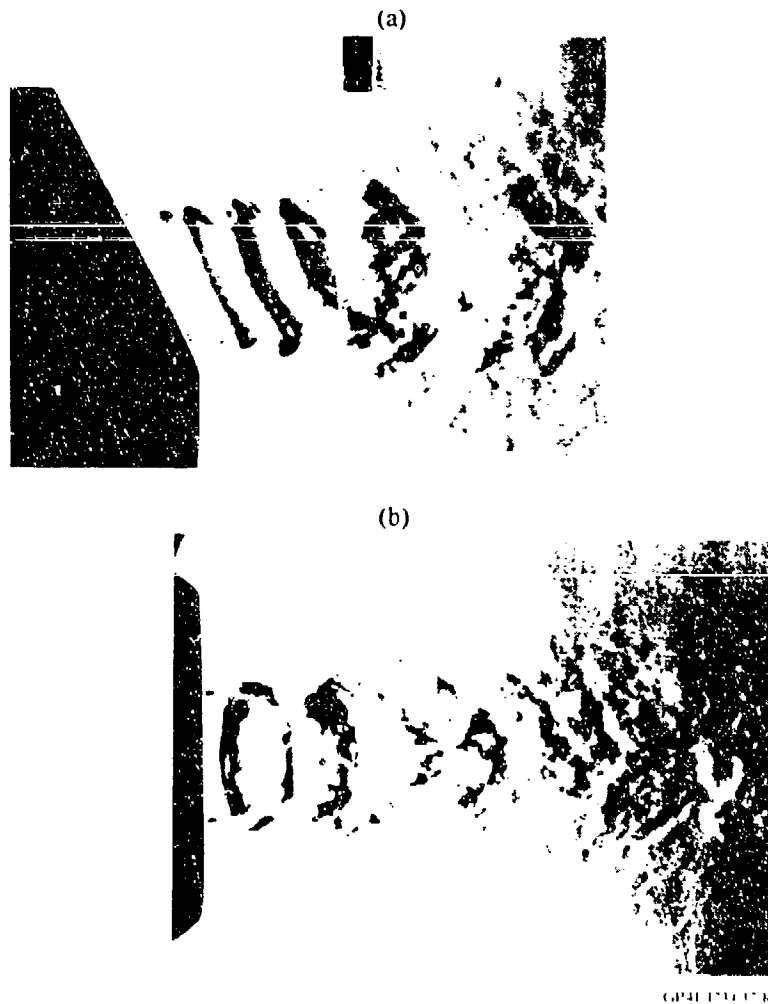


Fig. 5 Nozzle 1C;  $U = 30$  m/s, lip excitation:  $f_{ex} = 1390$  Hz.  
 (a) Side view and (b) view from  $\psi = 0^\circ$  (bottom).

themselves perpendicular to the mean flow direction. The orthogonal view in Fig. 5(b) shows a loop structure corresponding to the original vortex rollup and a subsequent complex interaction of vortices.

Figure 6 shows the tendency for a continuous vortex system that is initially coplanar with the nozzle exit to relax to an orientation normal to the jet. Even at the origin, the phase lines are not quite parallel and vortex-line bifurcations appear. Figure 6 represents a class of vortex interactions in which partially continuous vortex loops combine with each other in unequal numbers of pairings to orient the vortex system roughly perpendicular to the flow direction.

Figures 7-11 illustrate the large variety of vortex systems that can be generated from slanted nozzles by varying the slant angle, excitation frequency, and boundary-layer thickness. In Figs. 7-9 the primary variable is the frequency of excitation.

The flow presented in Fig. 7 for nozzle 2D shows a strong departure from the continuous vortex line system of Fig. 5. The distance to the initial rollup in the upper part of the photograph is greater than that for the lower

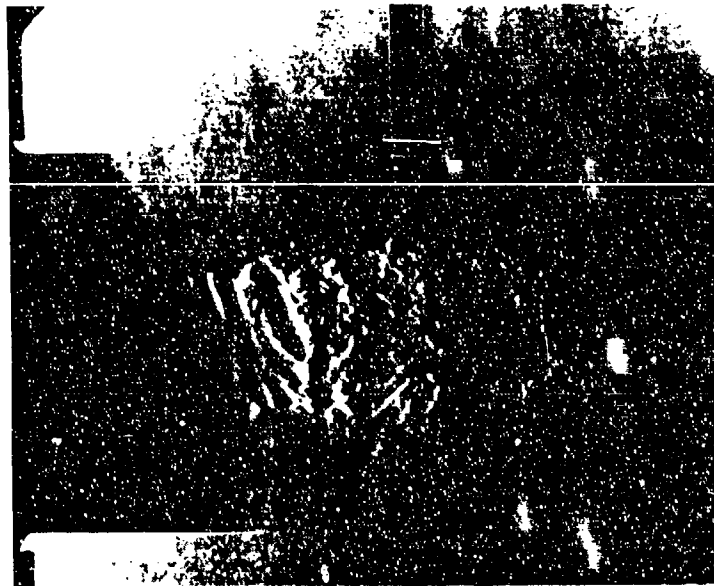


Fig. 6 Nozzle 1C;  $U = 30$  m/s, lip excitation:  $f_{ex} = 3230$  Hz.

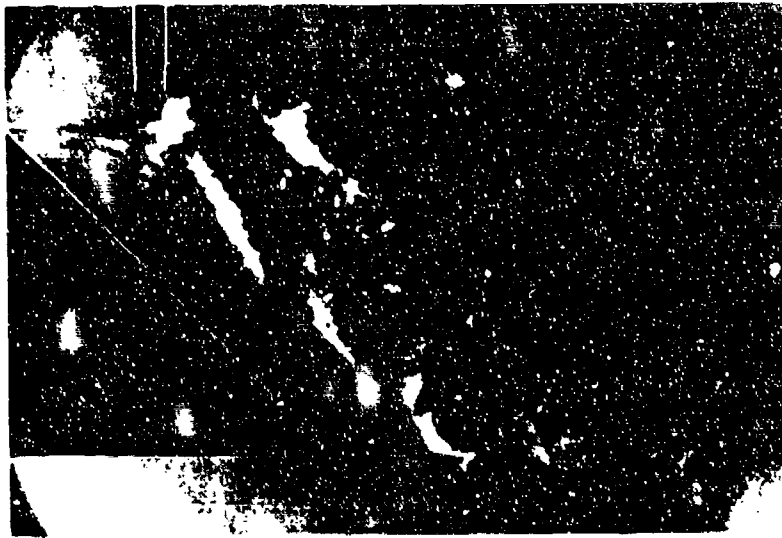


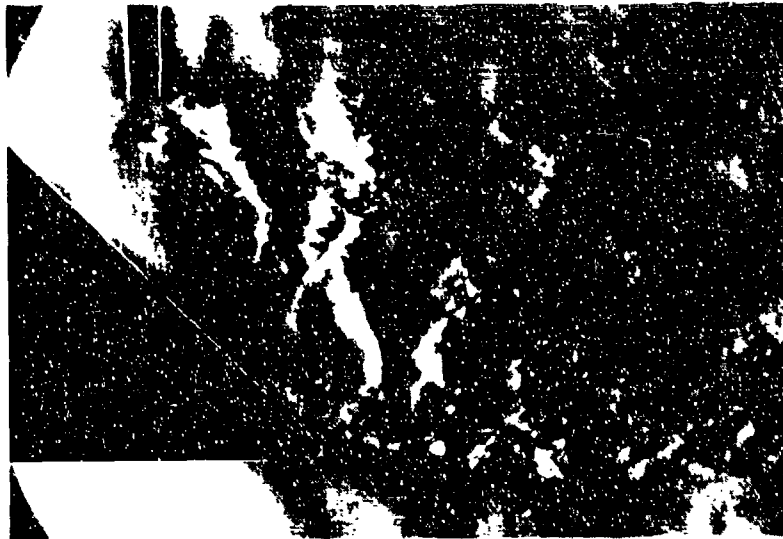
Fig. 7 Nozzle 2D;  $U = 25$  m/s, helium chamber excitation:  
 $f_{ex} = 364$  Hz.

shear layer. An intermediate vortex structure is visible at the azimuthal angle of approximately  $\psi = 90^\circ$ , corresponding to the side of the nozzle. Subsequently, a distorted vortex system that spans the entire flow is oriented at an angle halfway between that of the lip and the normal to the mean flow.

The flow shown in Fig. 8 demonstrates an even stronger tendency to form vortex systems that are perpendicular to the mean flow. It must be emphasized here that all the complex details of the flow visible in the photograph recur every time the strobe triggering conditions are satisfied.

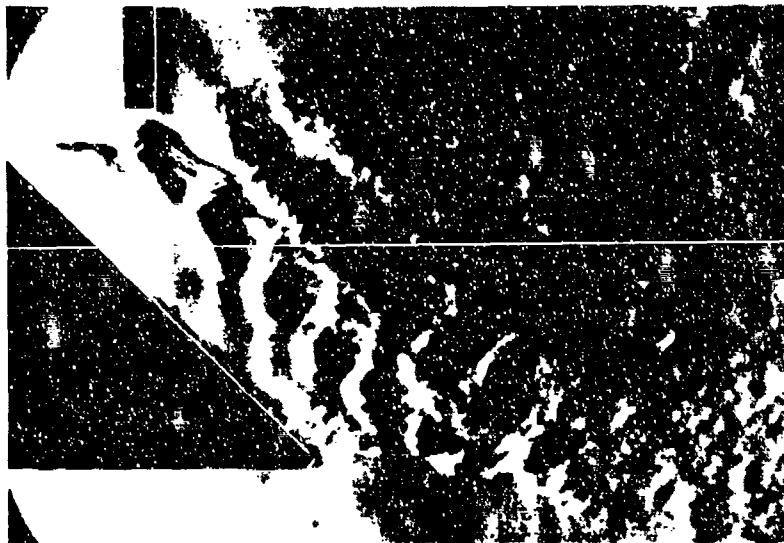
Figure 9 shows a superposition of two systems of instability waves, one generated parallel to the nozzle exit and another of much smaller wavelength, yielding a finer periodic structure along the constant-phase lines of the lower frequency wave. The conditions of the flow in Fig. 9 are identical to those presented in Fig. 8, with the exception of an increase in frequency from 450 to 475 Hz.

As the exit slant angles are increased, the fine structure visible in Fig. 9 can be demonstrated independently, as in Fig. 10 for nozzle 2E. The instability waves are initiated at  $\psi = 180^\circ$ , and the subsequent phase fronts are locally coherent for azimuthal angles that follow the slant of the nozzle termination with streamwise distance. This flow exemplifies the category of locally coherent instability-wave systems.



GP41-1734-6-R

Fig. 8 Nozzle 2D;  $U = 20$  m/s, helium chamber excitation:  
 $f_{ex} = 340$  Hz.



GP41-1734-7-R

Fig. 9 Nozzle 2D;  $U = 20$  m/s, helium chamber excitation:  
 $f_{ex} = 450$  Hz.

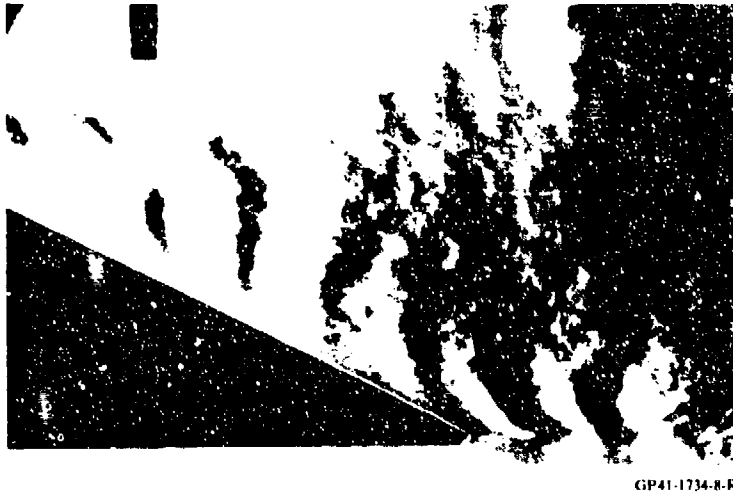


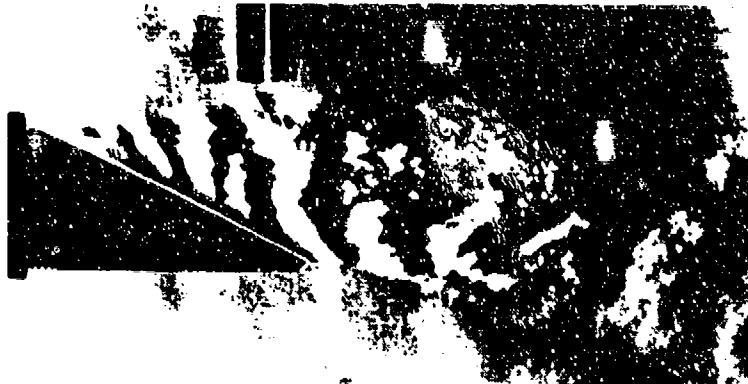
Fig. 10 Nozzle 2E;  $U = 15$  m/s, plenum excitation:  $f_{ex} = 475$  Hz.

Another version of an intermediate category of phase fronts is shown in Fig. 11 for nozzle 1E. In this instance the initial shear layer is thicker than in the previous figure and the resulting wave fronts span the full flow. The slant angle of the nozzle in Fig. 11 is the same as that in Fig. 10; however, the smaller nozzle size leads to an initial shear-layer thickness for which the ratio to the nozzle radius is approximately twice that of nozzle 2E in Fig. 10. The thicker shear layer has sufficient mass-weighted energy in the coherent motion of the instability wave system to allow the partially coherent initial instability waves to influence the entire flow and organize it into a system of vortices perpendicular to the flow axis, spanning the full flow width. In Fig. 10, for the thinner shear layer, the influence of the instability waves was limited to a sector of the flow for each successive, partially coherent wave segment.

### 3.5.3 Category II - Discontinuous I.O. Nozzles

We now consider a second category of flows--those with discontinuous origins. Each flow is generated by the merger of vortex systems that originate at the upper and lower lip lines of the stepped nozzles.

Figure 12 shows the flowfield for nozzle 2G. Plenum chamber excitation was used; therefore, the excitation wave may be taken to be an acoustic plane wave. The impingement of the wave on the lip of the upper sector, centered on  $\psi = 180^\circ$ , occurs effectively at the same time as that for the lower sector,



GP41-1734-10-R

Fig. 11 Nozzle 1E;  $U = 15$  m/s, plenum excitation:  $f_{ex} = 1078$  Hz.

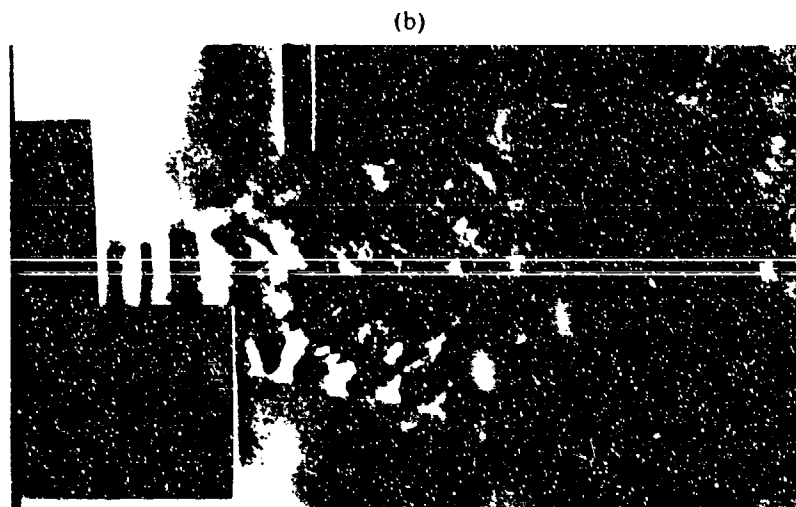
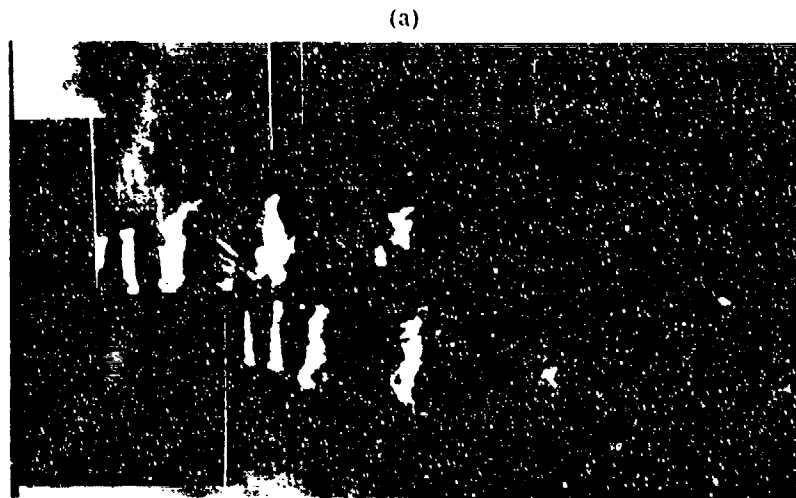


GP41-1734-9-R

Fig. 12 Nozzle 2G;  $U = 15$  m/s, plenum excitation:  $f_{ex} = 266$  Hz.

centered on  $\psi = 0^\circ$ , because the speed of acoustic propagation is more than an order of magnitude greater than that of the mean flow. The upper shear layer develops instability wave fronts perpendicular to the flow, analogous to that of the circular reference nozzle. Instability-wave formation for the lower sector, however, has been influenced by the upper one. Wave fronts of the lower sector begin to develop earlier with respect to their origin than those of the upper layer and interact with the more developed systems in the upper part of the flow. The result is a complex, asymmetric system of vortices for which the motion is repeatable with great fidelity.

In Fig. 13(a), the flow for nozzle 1G with an external excitation chamber is shown divided in the horizontal plane by a splitter plate which is visible



GP41 1734-11-R

**Fig. 13** Nozzle 1G;  $U = 15$  m/s, lip excitation:  $f_{ex} = 1199$  Hz. (a) With splitter plate and (b) without splitter plate.

as a line in the photograph. Both the upper and lower parts of the flow exhibit a sequence of vortex structures of increasing spacing, positioned in approximately the same sequence with respect to the local origin. When the splitter plate is removed, as in Fig. 13(b), the two parts of the flow interact, and the resulting vortex pattern appears qualitatively different from that in Fig. 13(a), although all other conditions remain unchanged. Figure 13 illustrates the role played by the full interaction of two vortex systems from separate origins in forming the global features of the flowfield.

If the frequency is changed, as shown in Fig. 14, then it is possible to obtain a vortex interaction pattern in which the upper and lower sectors of



GP41-1734-12-R

Fig. 14 Nozzle 1G;  $U = 15$  m/s, lip excitation:  $f_{ex} = 680$  Hz.

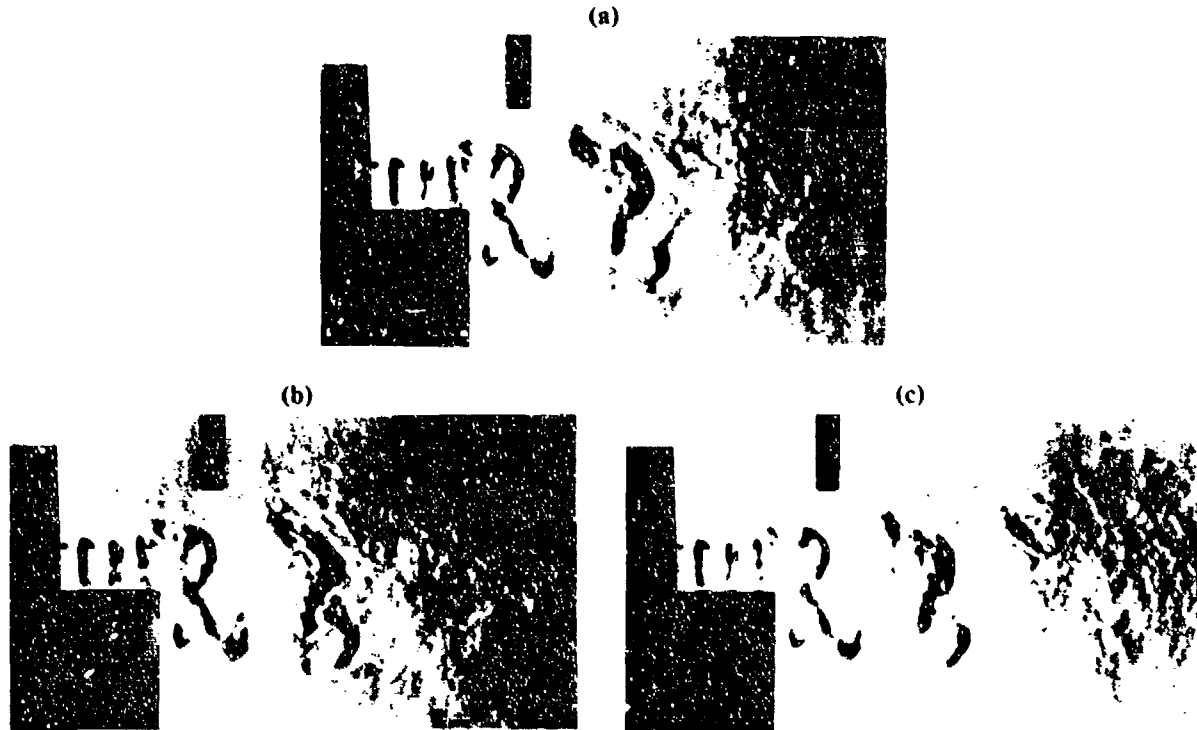
the flow are well synchronized, with a concurrent increase in the energy residing in the coherent flow.

In Fig. 15, the excitation frequency has been increased to 985 Hz. The series of three photographs demonstrates the complexity of three-dimensional interactions in this flowfield and, at the same time, shows the degree of repeatability of identical flow features in sequential cycles of vortex interaction. The degree of three-dimensionality in one photograph is sufficiently great to give the impression that the flow becomes random just downstream of the microphone position; however, when all three photographs are viewed, the repeatability of the structures is readily apparent. The videotape of the phase development of these structures highlights the fact that these complex flows are deterministic and repeat with great precision from cycle to cycle.

Figure 16 demonstrates a flowfield obtained by exciting only the upper sector of the shear layer. The two views of this flow describe the vortex patterns and demonstrate the disparity in spreading rates in the two perpendicular directions.

A small adjustment in frequency of excitation can result in large differences in spreading rates, as demonstrated by comparing Figs. 16 and 17. A change of only 17 Hz in excitation results in a large change in spreading angle of the upper part of the shear layer.

In Fig. 18, the upper and lower sectors of the excitation chamber are driven at the same frequency but with a 180-degree phase difference. The upper sector of the shear layer appears to be spreading by means of a sequence



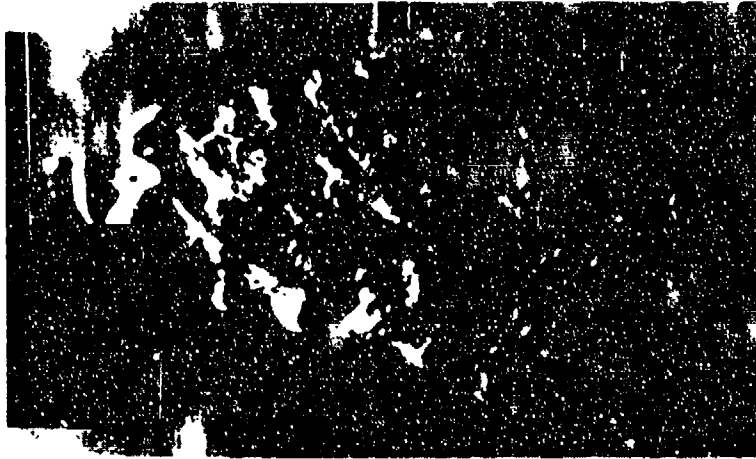
GP61-1193-4-R

Fig. 4. Step nozzle;  $U = 15$  m/s; lip excitation frequency  $f_{ex} = 985$  Hz,  $Re = 23\ 000$ : (a), (b), and (c) are three realizations of flowfields that meet identical conditioning criteria.

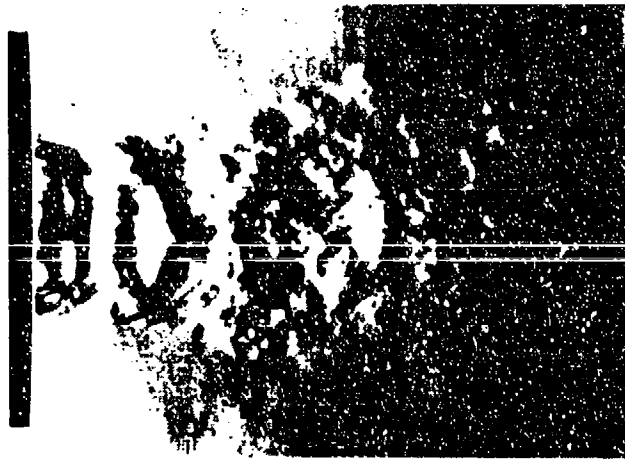
of vortex loops that are thrust out vertically; this flow represents cases in which large spreading rates were obtained by external forcing. The sequence of discrete loops that appear to be thrown out on an independent trajectory resemble the processes observed in the "blooming jet" experiments of Lee and Reynolds (Ref. 7). If the excitation for both upper and lower shear layers has the same phase, the effect is absent and a much lower spreading rate results.

Figure 19 shows results of a hot-wire survey of the flow described in Fig. 17. The data were taken at the axial station  $x/D = 4$ . Figure 19(a) presents the mean velocity as a contour plot, which is nonaxisymmetric with maximum spreading in the vertical direction. Comparison with similar flows without excitation reveals that excitation produces a larger degree of distortion than passive control of nozzle geometry alone. The azimuthal variation of momentum thickness is shown in Fig. 19(b). The measured momentum-thickness distribution reflects the vortex interactions visible in the corresponding flow-visualization photograph, Fig. 17. The ratio of momentum thicknesses of the top and the sides of the flow was approximately three.

(a)



(b)



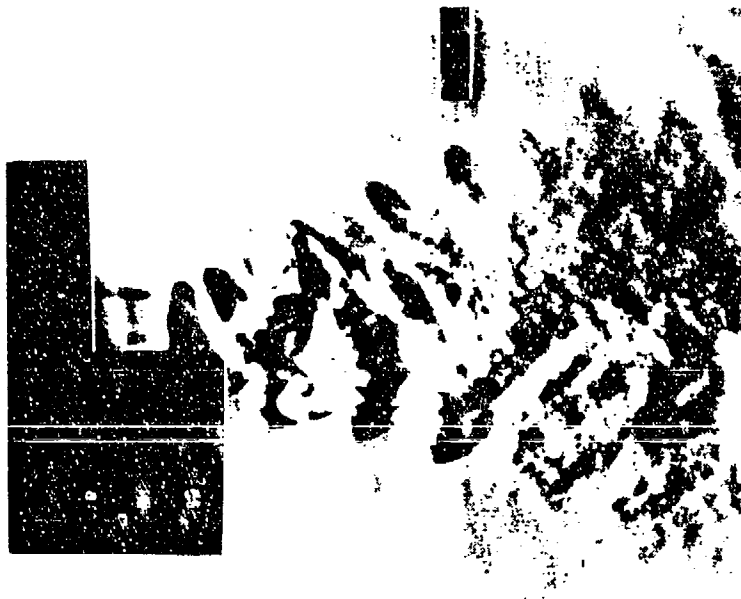
GP41-1734-14 R

Fig. 16 Nozzle 1G;  $U = 15$  m/s, lip excitation, upper sector only:  $f_{ex} = 428$  Hz. (a) Side view and (b) view from  $\psi = 0^\circ$  (bottom).



GP61-1931-R

Fig. 17 Nozzle 1G;  $U = 15$  m/s, lip excitation, upper sector only:  $f_{ex} = 411$  Hz.



GP41-1734-16-R

**Fig. 18** Nozzle 1G;  $U = 15$  m/s, lip excitation, upper and lower sectors  $180^\circ$  out of phase:  $f_{ex} = 411$  Hz.

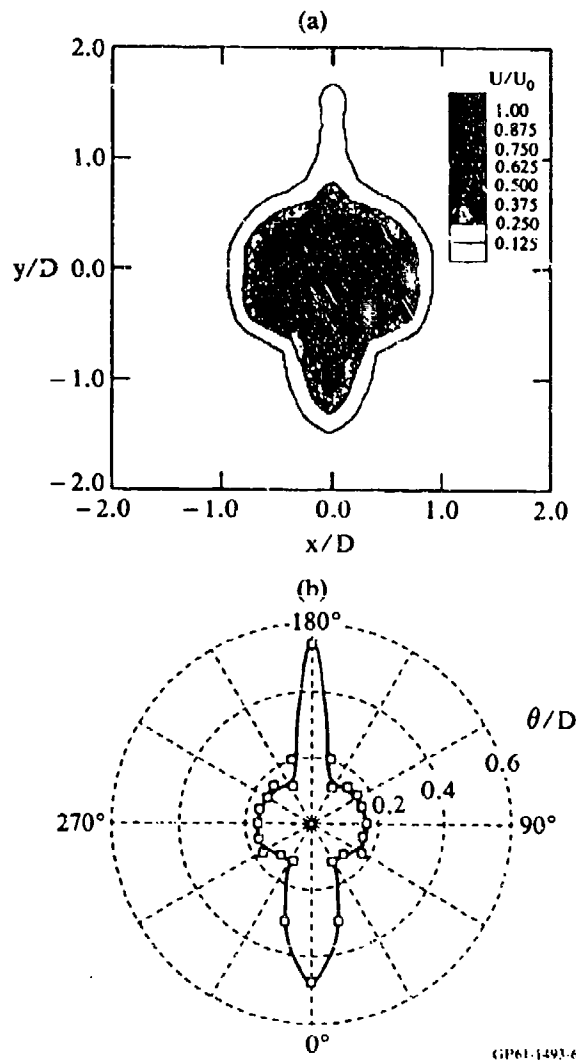


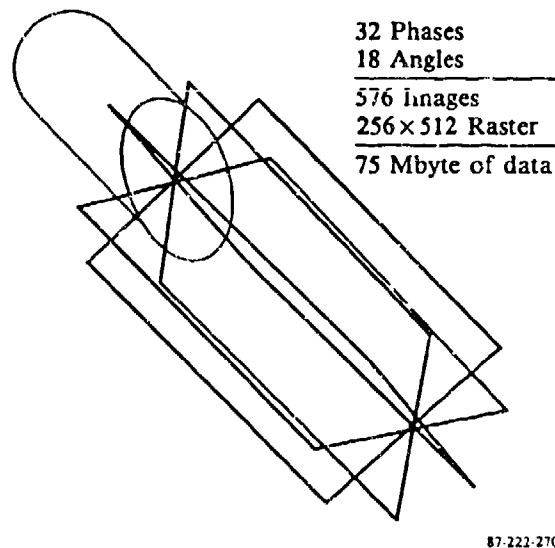
Fig. 19 Nozzle 1G;  $U = 15$  m/s, lip excitation, upper sector only:  $f_{ex} = 411$  Hz,  $x/D = 4.0$ ; (a) mean-velocity distribution and (b) momentum-thickness distribution.

## 4. INVESTIGATION OF SHEAR LAYER STRUCTURE

### 4.1 Image Acquisition

The three-dimensional structure of vortex lines in I.O. nozzle flows can be extracted from flow-visualization data, provided that a sufficient number of views of the flow from evenly distributed azimuthal viewpoints are obtained. The reconstruction is schematically illustrated in Fig. 20, which shows a series of flow-visualization planes taken at 18 different azimuthal angles; each flow visualization plane is photographed at 32 phase values of the primary wavelength of the periodically excited flow. The subsequent image processing stores 256 x 512 pixel images for each of 576 images, for a total of 75 Mbytes of data for one nozzle geometry at a single velocity and excitation condition.

The images are generated by phase-conditioned optical averaging, using a composite excitation process. The excitation waveforms superimpose the fundamental frequency and an additional waveform at the appropriate subharmonic, as shown in Fig. 21. Composite excitation permits locking of the large flow structure formation to the desired subharmonic and phase conditioning of the data with respect to the subharmonic.



87-222-270

Fig. 20 Three-dimensional reconstruction of vortex lines.

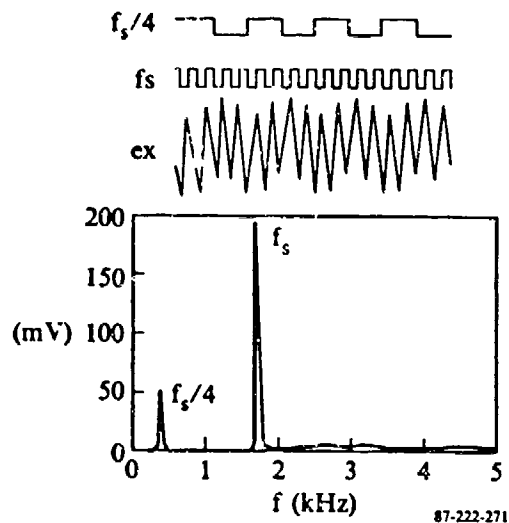


Fig. 21 Shear-layer composite excitation.

The entire pulsed-laser phase-conditioning system is shown in Fig. 22. A 20-W Cu-vapor laser, (Model 251, Plasma Kinetics, Inc., with 27-ns pulse duration and 6-kHz maximum repetition rate) controlled by a triggered input, generates a 6-cm-diameter beam which is spread in one direction by a cylindrical lens. The spreading is interrupted by a parabolic mirror, which generates a converging light sheet that is directed at the nozzle along the axis of symmetry of the flow system. A low-light-level RCA Ultricon video camera, operated at standard video rates, is used to average approximately 10 images per video frame. A high-resolution recorder provides stop-frame features for digitizing the images. A typical computer-enhanced image of a jet that has been seeded throughout the flow is shown in Fig. 23.

#### 4.2 Image Processing

Data from the Sony BVU820 video recorder were digitized at the facilities of the MDAC Image Processing Laboratory, which uses a Gould Deanza 8500 Image Processing system tied to a VAX 780 computer. The digitized images were locally enhanced to resolve the diffusion of tracer particles with streamwise distance. The dynamic range of the images has widened, the smoke intensity in the shear layer was effectively uniformly saturated throughout the image, and the vortices downstream appeared as bright as those upstream. Figure 24(a) shows a digitized image, and Fig. 24(b) shows the enhanced image after local

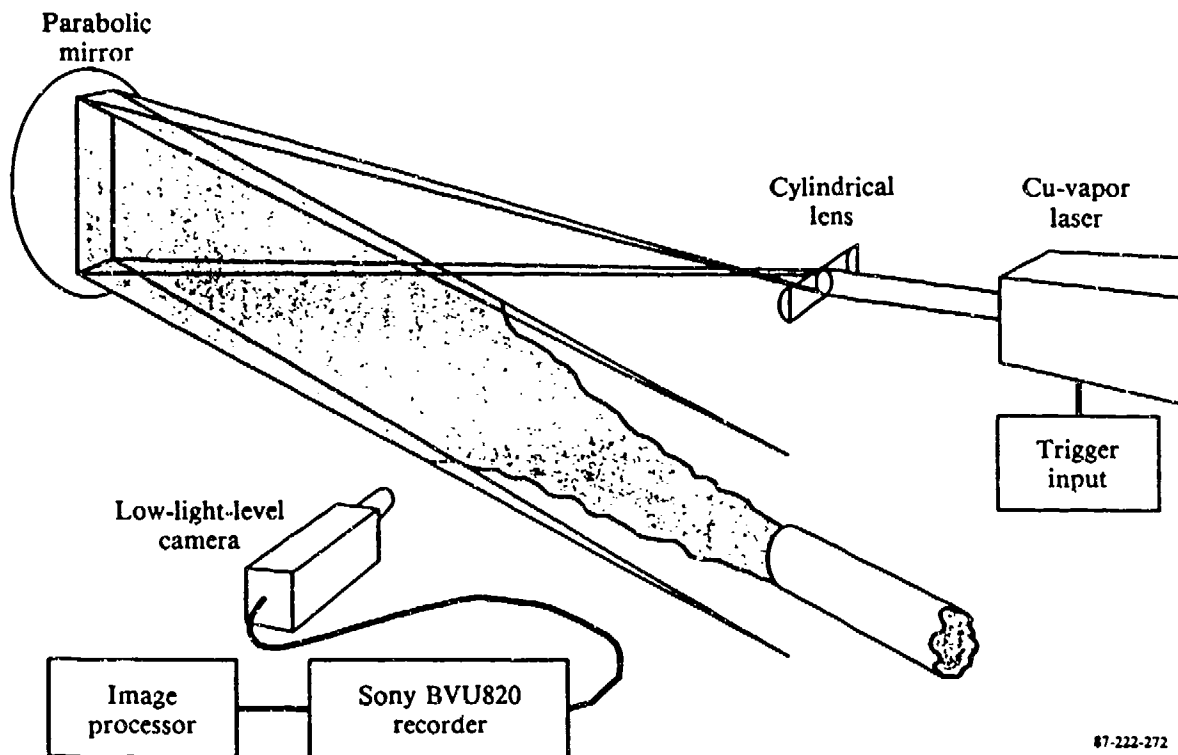


Fig. 22 Pulsed-laser flow visualization.

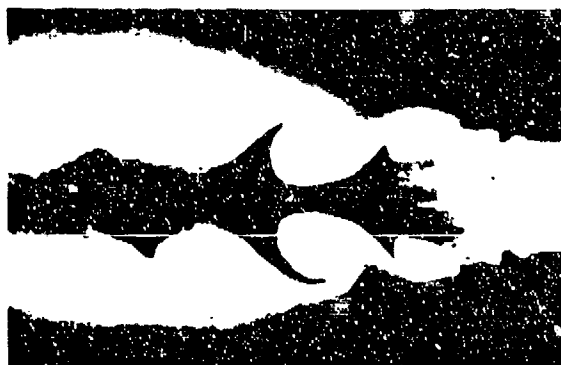


Fig. 23 Equalized image of seeded jet:  $U_0 = 22.5$  m/s;  $f_{ex} = 1736, 434$ .

equalization. An intensity threshold was used to detect the individual vortices. Figure 25(a) shows the binary image after the vortex-detection process, and the vortex locations in Fig. 25(b) were obtained by calculating the locations of the centroids of all independent intensity clusters. Separation of some of the bar-bell-shaped vortices into discrete vortices is one of the new improvements being developed in the technique.

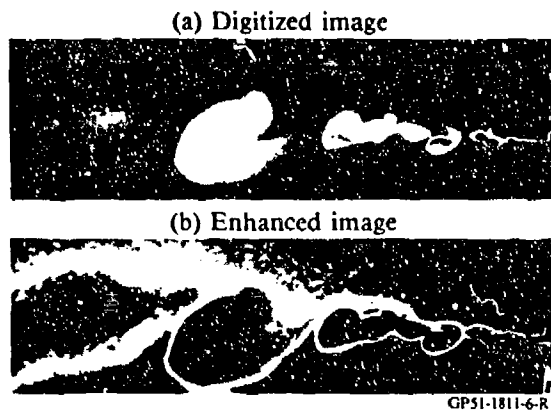


Fig. 24 Local histogram equalization technique.

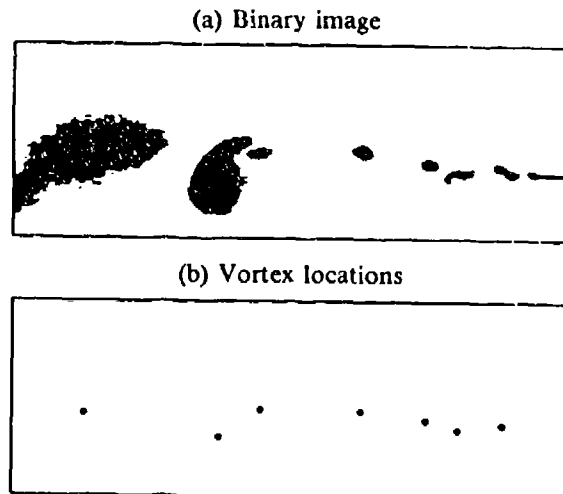


Fig. 25 Vortex detection.

The vortex core locations for each azimuthal plane were used to generate a series of vortex track diagrams. Streamwise and radial positions of the vortex cores were used to select pairing locations and to generate continuous vortex tracks as shown in Fig. 26.

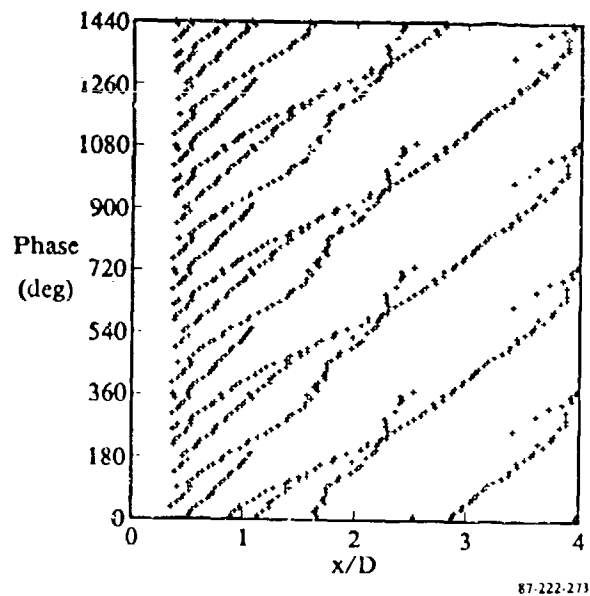


Fig. 26 Vortex track diagram; axisymmetric jet.

### 4.3 Image Display

The three-dimensional data file generated by the image-processing algorithms was downloaded to a Silicon Graphics IRIS 2400 work station (32-image bit planes, 8-Mbyte processor memory, 68020 processor, floating point processor, 272-Mbyte Winchester disk drive, Tektronix ink-jet printer, high-speed Ethernet connection to the VAX and capability for video-taping directly from the screen).

The calculated vortex tracks were converted into images showing vortex lines and the nozzle fully in three dimensions by use of the Graphix and MVIEW packages obtained from NASA Ames Research Center (ARC). The images may be rotated about arbitrary axes and viewed under arbitrary magnification. A succession of images may also be played back by using another software package obtained from NASA-ARC. This utility allows the images to be played back at a variety of speeds.

## 5. DISCUSSION AND CONCLUSIONS

The above results represent a survey of shear-layer spreading mechanisms related to initial geometry and excitation-parameter variation. These mechanisms result from the variety of three-dimensional, interacting vortex systems generated by I.O. nozzles and offer means for creating desired flow configurations through active control of initial conditions.

This report presents a selected subset of cases that we have explored and represents the beginning of an attempt to organize a variety of three-dimensional vortex interactions into a rational taxonomy. It is clear, however, that I.O. nozzle configurations offer controllable vortex systems whose interactions are sensitive to variations in initial geometry, excitation mode and frequency, amplitude, azimuthal phase distribution, and other applicable initial conditions.

Refined optical techniques, such as the phase-conditioned schlieren method reported here, can play an important role in surveying the full range of motions available for control. Refinement of these techniques also represents the initial step in collecting quantitative phase-conditioned information on the motion of complex three-dimensional vortex interactions. Such quantification involves image digitization and processing to emphasize salient features of three-dimensional systems evolving over time. Comparison of three-dimensional vortex systems associated with I.O. nozzles and the quasi-two-dimensional vortex interactions of the axisymmetric reference nozzle indicates that the large variety of available nozzle shapes and control modes results in flows that are different from conventional jet flows. Active control applied to I.O. nozzles appears to be an effective means of imposing a high level of order on coherent turbulent scales in shear layers, and therefore a technique that can be profitably employed for shaping flowfield development.

The pulsed-laser techniques used in this work offer a means of quantifying visualization results, by the systematic acquisition of visualization images with respect to the timing of significant repeating or conditionally selected flowfield events. The vortex-tracking procedure yields a quantitative description of interaction sequences that is not accessible through point measurements obtained with discrete sensors. The new high-resolution techniques for the monitoring of unsteady features of flowfields are needed to establish effective procedures for controlling flowfield dynamics.

## 6. PUBLICATIONS AND PRESENTATIONS

The following MDRL publications and presentations have resulted from the subject contract.

### 6.1 Publications

1. R. W. Wlezien and V. Kibens, "Passive Control of Jets with Indeterminate Origins," AIAA Journal, vol. 24, no. 8, August 1986, pp. 1263-1270.
2. V. Kibens and R. W. Wlezien, "Active Control of Jets from Indeterminate-Origin Nozzles," AIAA Journal (accepted).
3. V. Kibens and R. W. Wlezien, "Control of Jet Flowfield Dynamics," AFOSR-TR-84-0551, 1984.
4. R. W. Wlezien, "Quantitative Visualization of Acoustically Excited Jets," AIAA Journal (to be submitted).

### 6.2 Presentations

1. V. Kibens and R. W. Wlezien, "Instability Waves in Jets with Indeterminate Origins," Bull. Am. Phys. Soc. 28, 9 (1983).
2. R. W. Wlezien and V. Kibens, "Modification of Jet Flowfields by Passive Control," Bull. Am. Phys. Soc. 28, 9 (1983).
3. R. W. Wlezien and V. Kibens, "Passive Control of Jets with Indeterminate Origins," AIAA Paper 84-2299, 1984. Presented at the AIAA/NASA 9th Aeroacoustics Conference, Williamsburg, VA, 15-17 October 1984.
4. R. W. Wlezien and V. Kibens, "Shear-Layer Development of Jets from Crenelated Nozzles," 39th Annual Meeting of the Division of Fluid Dynamics, APS, Providence, RI, November 1984, (Bull. Am. Phys. Soc. 29, 9 (1984)).
5. V. Kibens and R. W. Wlezien, "Active Control of Jets from Indeterminate-Origin Nozzles," AIAA Paper 85-0542, 1985. Presented at the AIAA Shear Flow Control Conference, Boulder, CO, 12-14 March 1985.
6. R. W. Wlezien and V. Kibens, "Three-Dimensional Vortex Interactions in Excited Jets from Asymmetric Nozzles," 38th Annual Meeting of the Division of Fluid Dynamics, APS, Tucson, AZ, November 1985. (Bull. Am. Phys. Soc. 30, 10 (1985)).

7. V. Kibens, "Turbulence Control Research at MDRL," Joint Cal Tech/Stanford/ Industry/Government Workshop on Flow Control, Stanford University, April 1986.
8. R. J. Hakkinen, J. T. Kegelman, V. Kibens, F. W. Roos, and R. W. Wlezien, "Experiments on Turbulence Control in Jets and Shear Layers," presented at the IUTAM Symposium on Turbulence Management and Relaminarisation, Bangalore, India, 19-23 January 1987.

## 7. REFERENCES

1. Kibens, V. and Wlezien, R. W., Control of Jet Flowfield Dynamics, AFOSR-TR-84-0551, 1984.
2. Wlezien, R. W. and Kibens, V., Passive Control of Jets with Indeterminate Origins, AIAA Paper 84-2299, 1984.
3. Husain, H. S. and Hussain, A. K. M. F., Controlled Excitation of Elliptic Jets, Phys. Fluids, vol. 26, October 1983, pp. 2673-2765.
4. Gutmark, E. and Ho, C. M., Near Field Pressure Fluctuations of an Elliptic Jet, AIAA Paper 83-0663, 1984.
5. Krothapalli, A., Baganoff, D., and Karamcheti, K., On the Mixing of a Rectangular Jet, J. Fluid Mech., vol. 107, 1981, pp. 201-220.
6. Breidenthal, R., Response of Plane Shear Layers and Wakes to Strong Three-Dimensional Disturbances, Phys. Fluids, vol. 23, Oct. 1980, pp. 1929-1934.
7. Lee, M. J., and Reynolds, W. C., Structure of the Bifurcating Jet, Bull. of the Am. Phys. Soc., vol. 28, Nov. 1983, p. 1362.
8. Rockwell, D., Invited Lecture: Oscillations of Impinging Shear Layers, AIAA Paper 82-0047, 1982.
9. Smith, C. R., Three-Dimensional Recreation of the dynamic Motion of a Single Hydrogen Bubble-Line, Bull. Am. Phys. Soc., vol. 28, Nov. 1983, p. 1405.
10. Kibens, V., Discrete Noise Spectrum Generated by an Acoustically Excited Jet, AIAA J., vol. 18, April 1980, pp. 434-441.
11. Roshko, A., On Organized Motions in Turbulent Shear Flows, Bull. of the Am. Phys. Soc., vol. 28, Nov. 1983, p. 1401.